LAB 06

TRANSMISSION ELECTRON MICROSCOPY

REPORT BY: SHILPIKA CHOWDHURY

TEAM MEMBER NAME: Henry Geerlings, Ashley Tsai, Chris Chuang, Sam McAlpine
LAB SECTION No. 105 GROUP 2

EXPERIMENT DATE: April 22, 2014
SUBMISSION DATE: May 6, 2014

ABSTRACT

The goal of this experiment was to identify the relationship between transmission electron microscope (TEM) diffraction and bright field image in the JEOL® JEM 2011 transmission electron microscope. Further, we characterized the rotation caused as a result of magnification. After measuring the difference in angle between the bright field image and the diffraction patterns, it was found that only a slight clockwise rotation appeared in negligible scales. Thus, the manufacturer's claim for rotation-free viewing was valid.

INTRODUCTION

Transmission Electron Microscopes (TEM) image a sample by accelerating electrons *through* a very thin sample and recording the location and intensity of transmitted beam on the detector[2]. The magnification of these microscopes can range from 40x to more than 50,000x. TEM presents many opportunities to visualize a sample in suspension or even sample that has been grown on the imaging surface, such as MoO_3.

TEM grids are traditionally 3 mm diameter perforated disks with anywhere from 50 to 400 holes (called the mesh of the grid). These disks often have a film of carbon placed on them in order to provide a surface on which the sample (usually smaller than the hole width) can sit. Unlike the thicker metal of the grid, which absorbs most of the electrons that strike it, a thin carbon film allows electrons to be transmitted and recorded. This sample is loaded into the microscope column, and an electron source will emit electrons to be accelerated through the sample along the column.

There are multiple planes in the column of the TEM, one of which is the image plane on which an image of the sample can be seen and another is the back focal plane. There are multiple lenses inside the column of the TEM as well, which determine which of the planes are in focus. The objective lens brings images into focus, and a microscope operator can control condenser lenses to change the amount and orientation of light hitting the sample. When the back focal plane is in focus, we are able to see a diffraction pattern. The diffraction pattern of a crystalline sample can be used to not only determine periodicity of the sample but also to determine crystal orientation.

During the manipulation of a magnetic lens, the trajectory of the voltage accelerated electrons takes on an additional perpendicular acceleration resulting in a helical path. This path can result in rotation of a bright field image as magnification of the image is increased. During the use of a diffraction pattern and a bright field image in accordance, it is essential to take into account the rotation caused during image magnification as a diffraction pattern will not be subject to the same rotation as a bright field image. The difference in rotation can be documented and the microscope calibrated in order to correct for the error.

The thin film sample MoO_3 is particularly useful for rotation correction due to the ease with which it can be deposited onto a grid and the orthorhombic structure of the crystal. The orthorhombic crystal diffraction pattern is pronounced, diffracts at all lattice points and the axis directions can easily be seen, allowing for simplified alignment along the broad faces of the diffraction pattern.

In the JEOL® JEM 2011 microscope, no rotation is expected due to a manufacturer claim that intermediate and projector lenses have special rotation limiting current control.

EXPERIMENTAL PROCEDURES

In this experiment, a JEOL® JEM 2011 Transmission Electron Microscope was used to collect diffraction and bright field images from a thin Molybdenum Trioxide (MoO_3) crystallite on thin carbon film 200 mesh copper grid produced by Ted Pella Inc.

BRIGHT FIELD IMAGE COLLECTION

The MoO_3 sample was loaded into an evacuated TEM column. The sample's zone axis was expected to already be correctly oriented, so tilting was omitted from the procedure. Then, bright field images were taken at various magnifications (12,000x, 20,000x, 40,000x, 60,000x, 80,000x, 100,000x, and 120,000x) and corresponding diffraction images were taken at each point. Image collection was facilitated through a CCD camera interface similar to Digital Micrograph.

DIFFRACTION PATTERN COLLECTION

As mentioned previously, diffraction images were taken at each magnification with a bright field image. Diffraction patterns were taken at a height of 40 cm for all images, and the sample was moved within the field in order to optimize diffraction pattern.

EXPERIMENTAL RESULTS

At each magnification, first a bright field image of the sample was taken then a diffraction pattern was collected. Each image is shown below. The angle between the broad axis and the bright field image edge is tabulated for each sample at the end of the section.

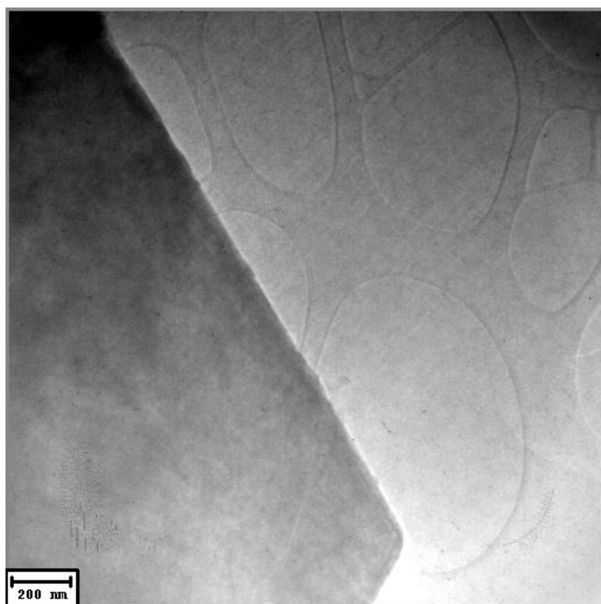

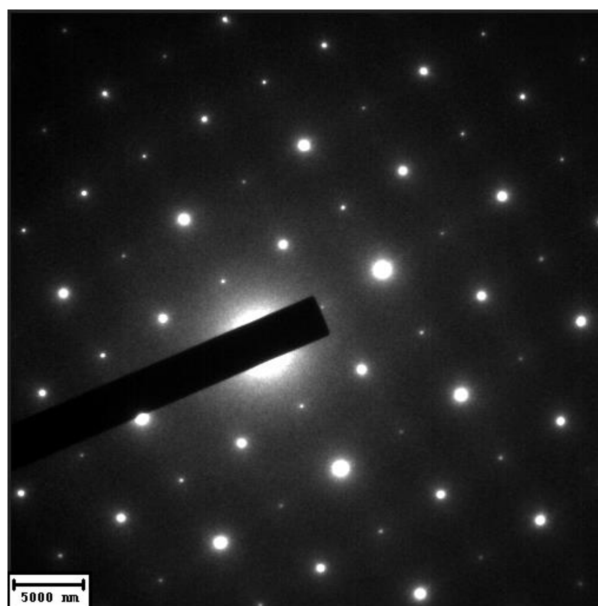

Figure 1: Images of MoO_3 at 12,000x magnification. On the left, a bright field image with a characteristic angle. On the right, the corresponding diffraction image for the sample, without rotation.

The angle between the broad axis and the bright field image is listed in Table 1.

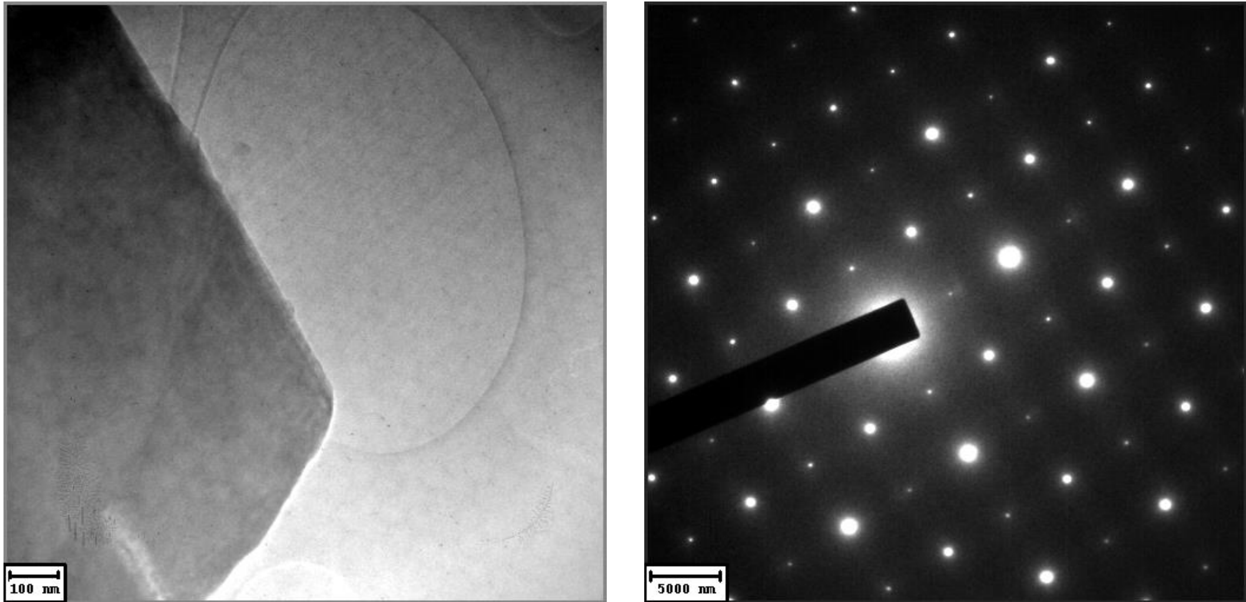

Figure 2: Images of MoO_3 at 20,000x magnification. On the left, a bright field image with a characteristic angle. On the right, the corresponding diffraction image for the sample, without rotation. Without measurement, little rotation is visible.

The angle between the broad axis and the bright field image is listed in Table 1.

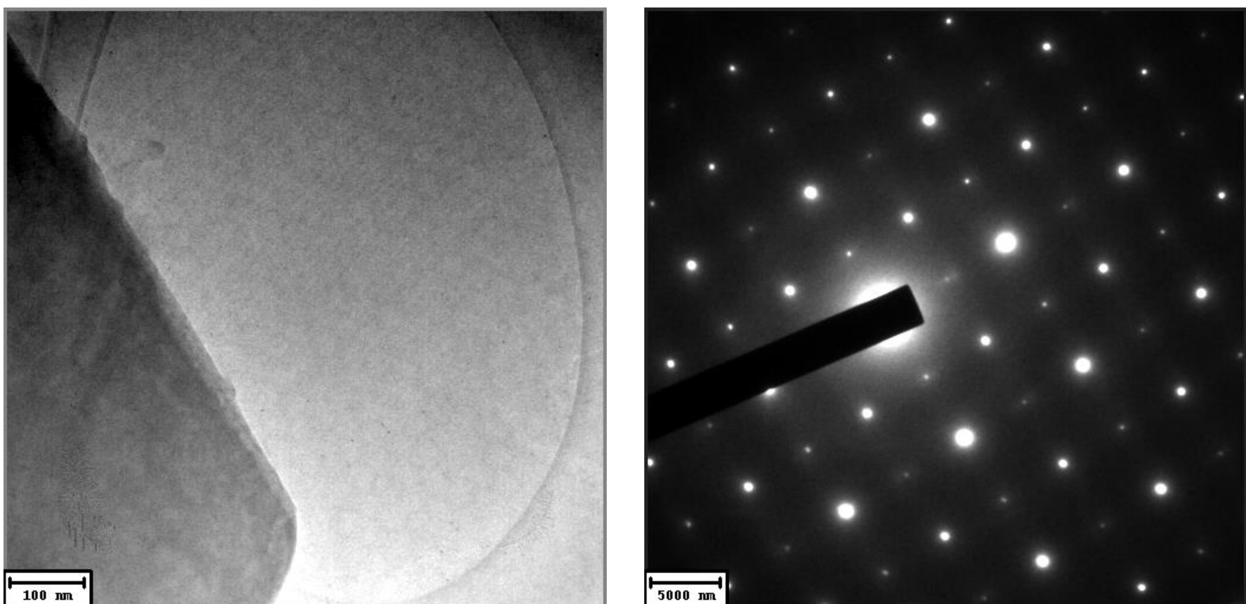

Figure 3: Images of MoO_3 at 40,000x magnification. On the left, a bright field image with a characteristic angle. On the right, the corresponding diffraction image for the sample. The sample background carbon film may be contributing to the smaller spots in the diffraction pattern.

The angle between the broad axis and the bright field image is listed in Table 1.

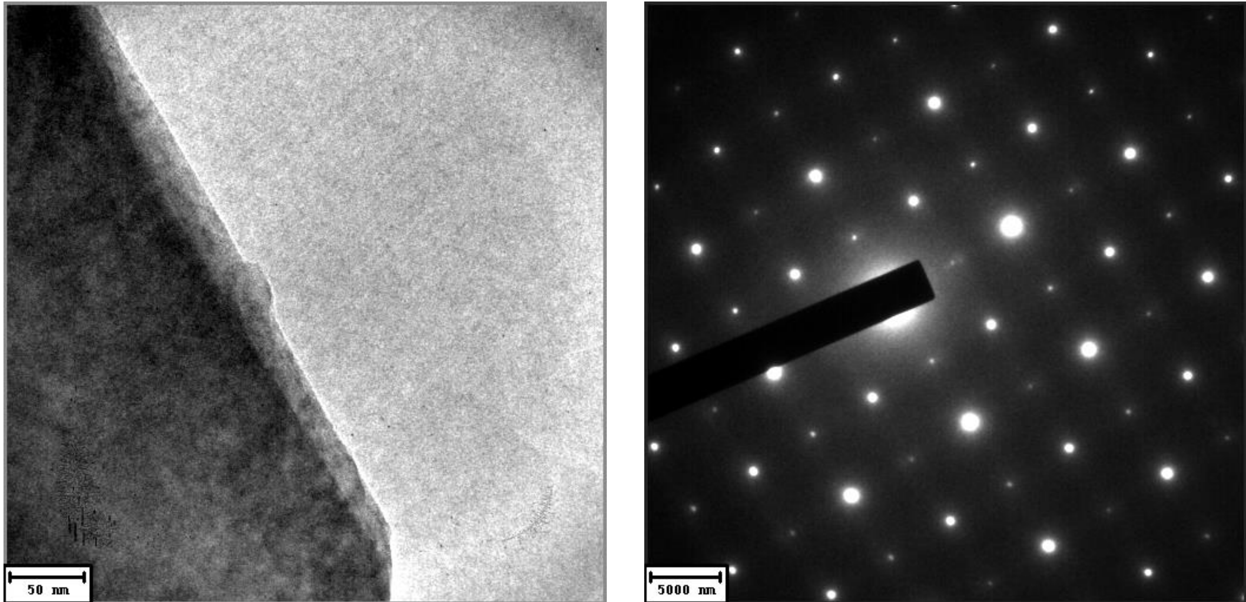

Figure 4: Images of MoO_3 at 60,000x magnification. On the left, a bright field image with a characteristic angle. On the right, the corresponding diffraction image for the sample. Only the region nearest the corner was used for angle measurement, not the entire crystal edge.

The angle between the broad axis and the bright field image is listed in Table 1.

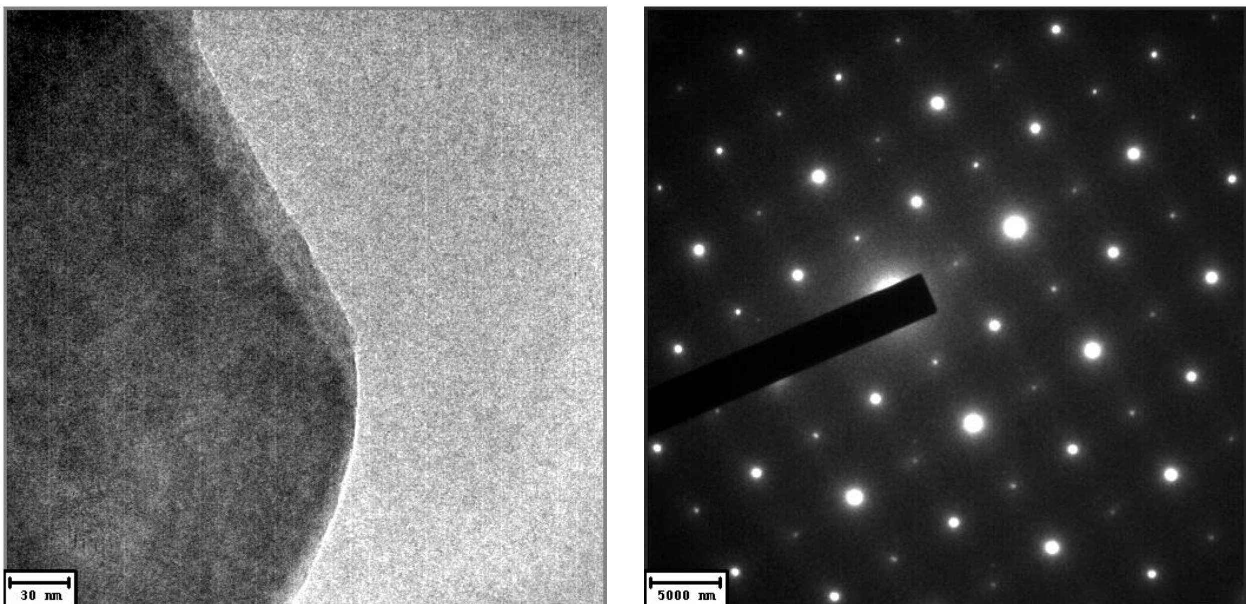

Figure 5: Images of MoO_3 at 80,000x magnification. On the left, a bright field image with a characteristic angle. On the right, the corresponding diffraction image for the sample, without rotation.

The angle between the broad axis and the bright field image is listed in Table 1.

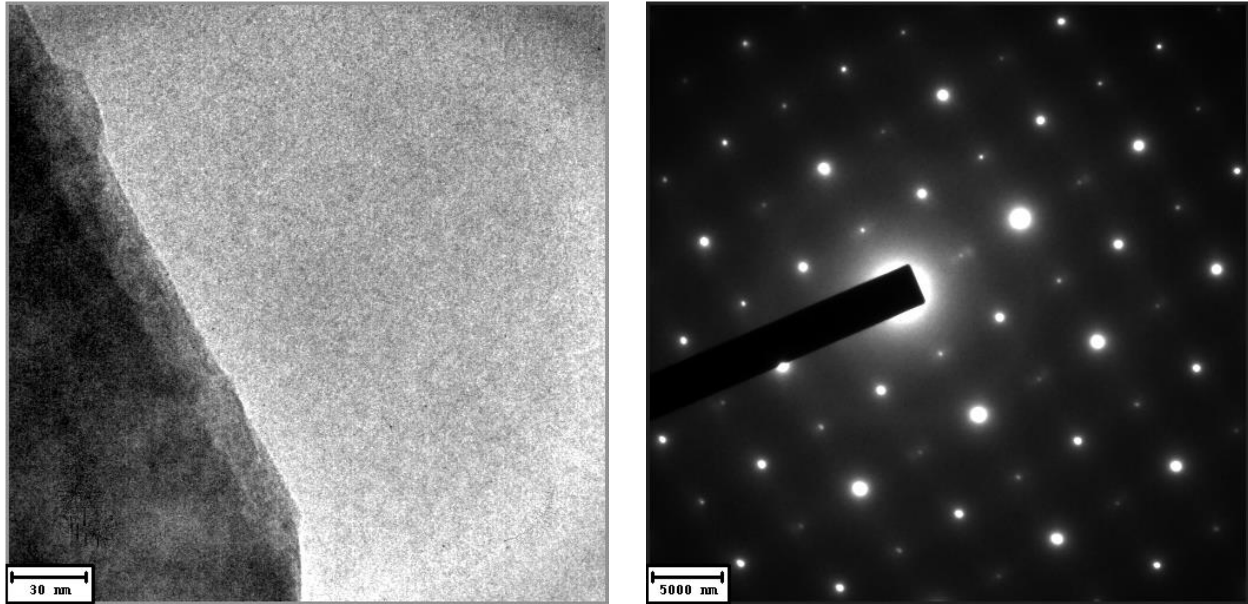

Figure 6: Images of MoO_3 at 100,000x magnification. On the left, a bright field image with a characteristic broad angle. On the right, the corresponding diffraction image for the sample. Lacy film is no longer visible in the bright field image.

The angle between the broad axis and the bright field image is listed in Table 1.

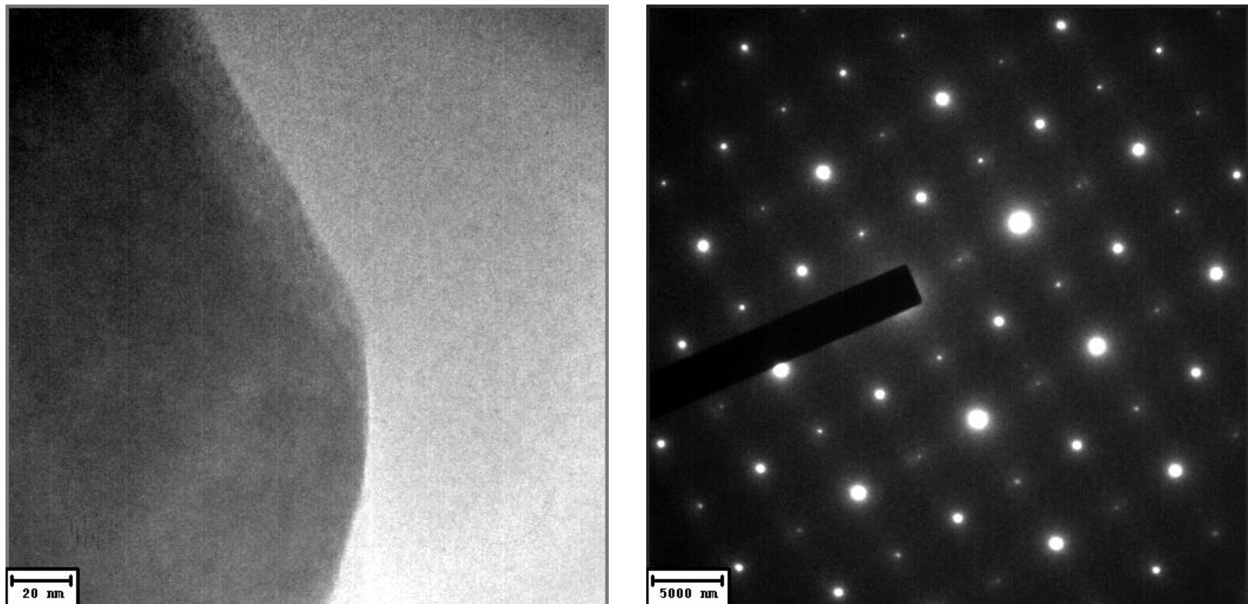

Figure 7: Images of MoO_3 crystallite at 120,000x magnification. On the left, a bright field image with a characteristic angle. On the right, the corresponding diffraction image for the sample, without rotation.

The angle between the broad axis and the bright field image is listed in Table 1.

Table 1: Tabulated rotation data. Angles are measured in degrees away from the vertical. The bright field angle was calculated as the edge of the crystal. The diffraction angle was calculated compared to the line formed by the broad edge diffraction points.

Magnification	12,000x	20,000x	40,000x	60,000x	80,000x	100,000x	120,000x
Bright Field	28.61°	28.71°	28.61°	28.75°	28.93°	28.31°	28.34°
Diffraction	32.01°	32.29°	32.03°	32.28°	32.06°	32.36°	32.51°
Difference	3.4°	3.58°	3.42°	3.53°	3.13°	4.05°	4.17°

Figure 8: Below, the diffraction pattern of crystal tilted to ideal perfect zone axis orientation. This was done in order to compare the ideal zone axis with the experimental alignment in diffraction. It is clear to see that the perfect zone axis image has more uniform spots on the image, but maintained the same broad angle alignment.

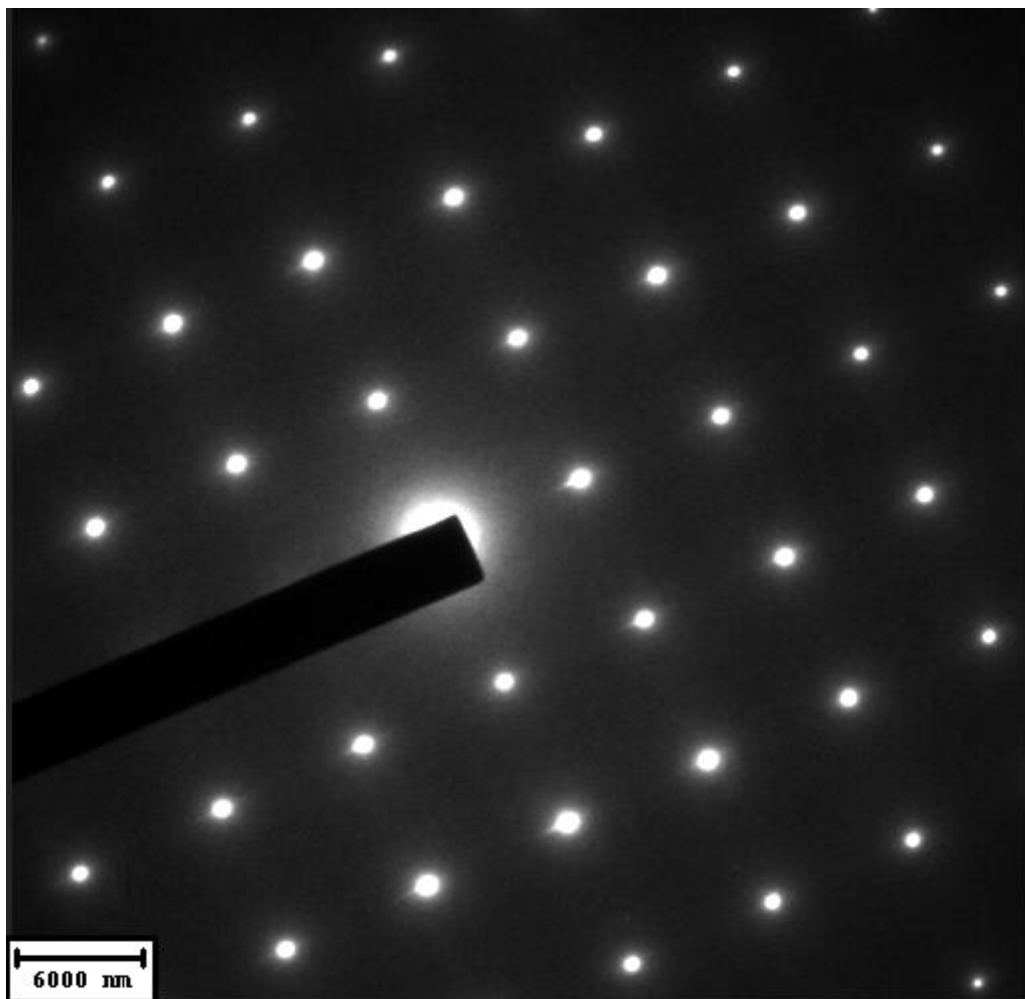

DISCUSSION

The data was used to evaluate the degree of rotation in the machine despite advertised correction for helical electron trajectory.

DATA ANALYSIS

INDEXING AND ZONE AXIS

The perfect zone axis image, Figure 8, displays the symmetry that results from diffraction. A zone axis is observed if the reciprocal space plane is normal to the momentum vector of the incident electrons, creating a uniform brightness array of spots in the orthorhombic system at the center of the diffraction pattern. Lighter spots at the edges of the pattern are due to higher order Laue zones, described by an Ewald Sphere construction with an extremely large radius.

Despite being orthorhombic in lattice, the crystal has a symmetry that makes the broad angle relative to any reference direction. Figure 9 has the diffraction spots labeled as [100], [010], with [001] in the direction normal to the plane of the image[1]. These points are labeled as locations *on* the reciprocal lattice, not as the real lattice from which they map.

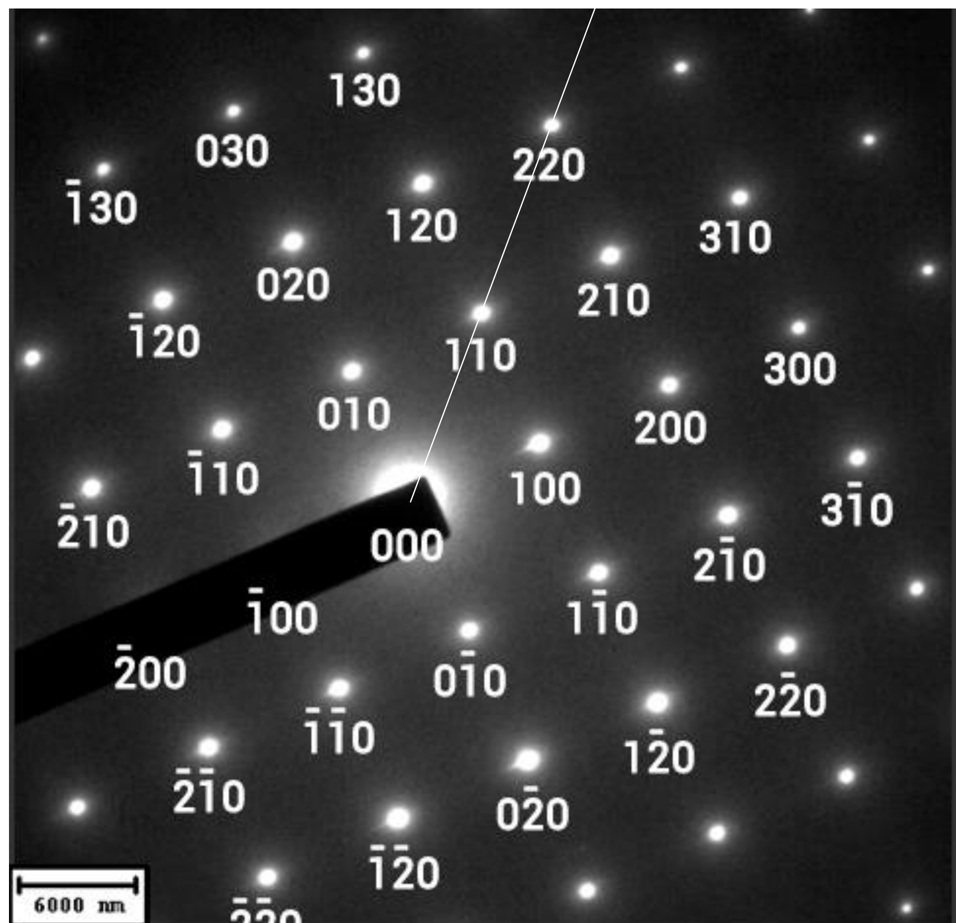

Figure 9: The diffraction pattern of crystal tilted to the perfect zone axis orientation with indexing shown.

On the image, a light line indicating the habit plane used for orientation is shown.

HABIT PLANE

The habit plane is the plane across which twinning occurs. For the calculation of the angle changes the direction [110] in the system described in Figure 9 was used across which twinning would occur. This is because across this direction, the lattice is most inclined to form twin planes, a defect in the system.

DATA REDUCTION

MAGNIFICATION INDUCED ROTATION

Using the data from Table 1, a plot can be made relating magnification to angular shift between the bright field images and the broad diffraction spots. Figure 10 shows the results of plotting angular difference versus magnification. A very slight change in angle can be seen as magnification increased (so small that it may be negligible) but it appears the image is rotated in a clockwise direction. This change is so slight, however, that the manufacturer's claim that rotation free magnification is true. The R^2 value of the data does not show enough correlation to describe a certain change in angle.

Figure 10: Plot of angle between bright field image edge and broad plane line from corresponding diffraction pattern. The angle appears to be increasing with increased magnification, indicating a clockwise rotation with increased magnification. After fitting the line, it appears that the change in rotation is extremely small. The rotation will only change 6 degrees for degree 10^6 change in magnification, which is higher than what we expect to achieve with this microscope.

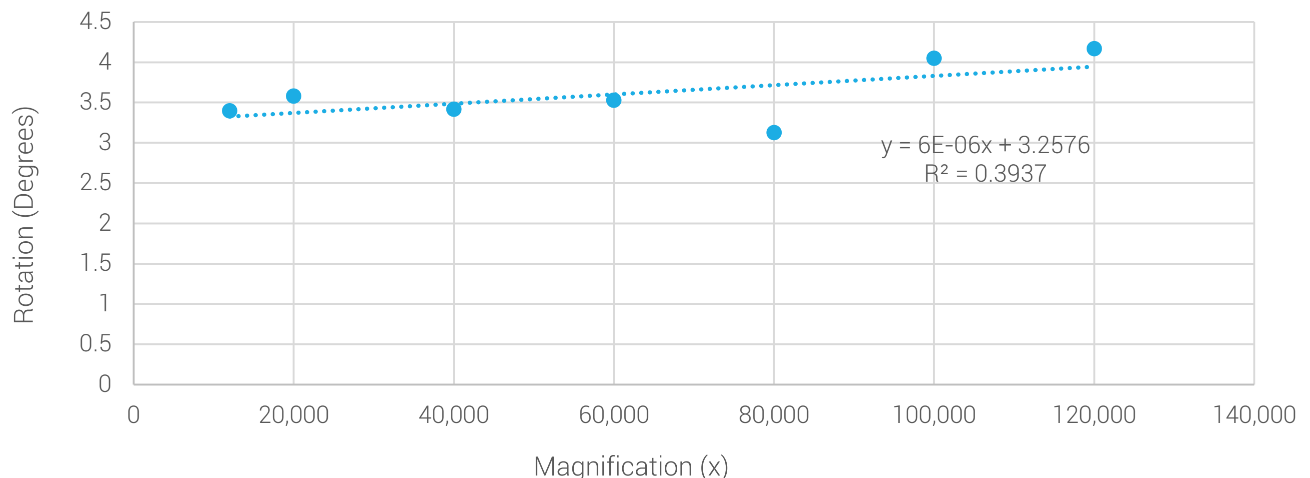

ERROR SOURCES

The main source of error in this experiment would have been during the relative angle calculation. The method used in this data analysis was rotation with Adobe Photoshop © until the axis of interest was aligned with the vertical. Then, the angle needed to achieve this vertical orientation was recorded. Human errors may have occurred when visually aligning the centers of the spots with the vertical, however the slight departure from a perfect zone axis allowed for more accurate

centering of the vertical as interstitial diffraction points were smaller and therefore improved center-point approximation.

CONCLUSIONS

From this lab we concluded that negligible clockwise bright field rotation is observed when imaging with a JEOL® JEM 2011 Transmission Electron Microscope, upholding the manufacturer's claim regarding "rotation-free" imaging.

REFERENCES

[1] "DoITPoMS." - TLP Library Indexing Electron Diffraction Patterns. N.p., n.d. Web. 06 May 2014. http://www.doitpoms.ac.uk/tlplib/diffraction-patterns/printall.php

[2] B.D. Cullity and S.R. Stock, Elements of X-Ray Diffraction, 3rd Edition, Prentice-Hall, New York, (2001), p. 418.

[3] R. Gronsky. Lab 06 Manual: Transmission Electron Microscopy. MSE 104. University of California Berkeley, Berkeley, CA.